

## Robust Inverse Dynamics Control and Vibration Rejection for Inertial Stabilization Systems

Sangveraphunsiri V. and Malithong K.

Department of Mechanical Engineering, Faculty of Engineering, Chulalongkorn University  
254 Phyathai Patumwan Bangkok 10330 Bangkok, Thailand, 10330  
Corresponding Author: Tel: 0-2218-6449, Fax: 0-2218-6583,  
E-mail: [viboons.s@eng.chula.ac.th](mailto:viboons.s@eng.chula.ac.th)

### Abstract

This paper presents a controller that satisfies stabilization performance of an inertial stabilization system. This system has a 2-DOF gimbal which will be attached to an aviation vehicle. The camera is mounted at the center of the gimbals' inner joint. Our previous works in controller design, the robust inverse dynamics control and the line of sight (LOS) stabilization, are used for compensation of the nonlinearities, model uncertainties, and disturbances from environment. Although our mechanisms are carefully designed with statically balance, the system still has dynamic unbalance. The center of the gravity will shifted due to the configuration change during tracking and moving of the gimbal relative to a carrier. This will induce acceleration, forces due to mass unbalance of the gimbal. These effects will be classified as disturbance torque to the input and need to be suppressed. This disturbance torque can be eliminated by the angular and angular rate feedback but a better method can be revised. Since the acceleration of the moving platform, due to the disturbance torque, can be measured, a feedforward disturbance rejection can be generated to compensate the disturbance torque. The experimental results confirm the validity of the control design procedure for the two-axis gimballed stabilization system. The proposed controller is capable enough to overcome the disturbances and the impact of LOS disturbances on the tracking performance

**Keywords:** Inertial stabilization system / robust inverse dynamics control / acceleration feedforward

### 1. Introduction

In motion control of the inertial stabilization system, the sources of uncertainties are inertia, damping friction, vehicle motion, structural flexure and disturbance torque. Although disturbances arise from many sources, the net effect can be described by an equivalent torque disturbance  $T_d$ , which simplifies gimbal mathematical modeling. A Major problem in inertial stabilization systems is the rejection of disturbances associated with moving components. There are many works that have been done in this area, such as a nonlinear induced disturbance rejection is purposed in [5], Adaptive Fuzzy PID controller for LOS stabilized system is purposed in [4]. Robust inverse dynamics and Sliding mode control with indirect line of sight stabilization [1] are purposed in [3]. Feedback stabilization based on combination of the mass stabilization and measurements of inertial angular rates were surveyed in [2].

A major source of uncertainties is mass imbalance of the payload. Imbalance produces LOS jitter when the payload center of gravity is

not centered on an axis of rotation for the gimbals. Therefore linear vibration produces torque disturbances. Consider unbalance mass system revolved around a central axis  $O$ , as shown in Fig. 1. The geometry is sketched for a single axis of rotation orthogonal to the direction of acceleration (the vertical direction). The unbalance is represented by an eccentric mass  $M$  with eccentricity  $r$  that is rotating with angle  $q$ . The case of an elevation joint is composed of both the gravitational  $g$  and the translational acceleration  $a$ . Force  $F$  generated by the unbalance mass  $M$ .

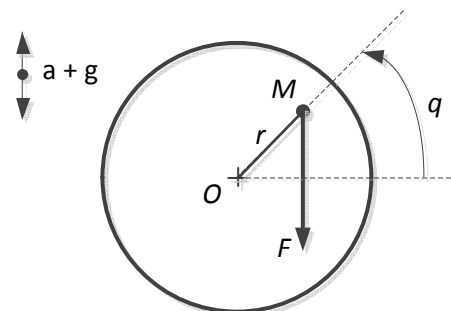


Fig. 1 Free body diagram for the case of an elevation joint

This paper focuses on the controllers, the robust inverse dynamics control [6] and acceleration feedforward that takes advantage of robustness with respect to model uncertainties and disturbances, for stabilizing the servo loop. Fig. 3 shows the block diagram of the robust inverse dynamic control and acceleration feedforward. An inertial measurement sensor is added to detect vehicle angular rate and orientation for outer loop control and an accelerometer is added to detect vehicle's linear acceleration.

## 2. Dynamic Model of inertial stabilization system

The inertial stabilization system consists of two outer joints and two inner joints. In Fig. 2, the payload is mounted at the center of the inner joints. These joints have a freedom to move a few degrees and will prevent high frequency rotational vibrations to reach the camera. These frames are kept at the center position by magnetic field, so that shock vibration will be damped out effectively. The outer joints consist of the azimuth axis and the elevation axis. Both axes are controller by DC Servo motors. Two encoders measure the pan and tilt angles for the both axes.

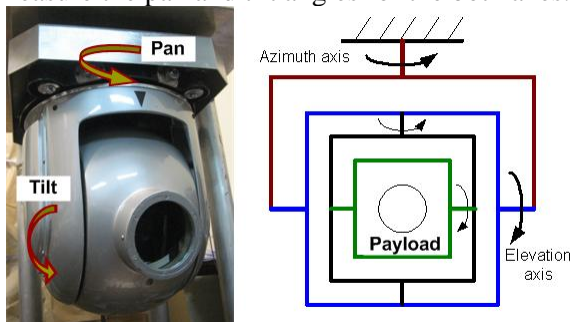


Fig. 2 The inertial stabilization system configuration

The dynamic model of the inertial stabilization system can be written in the joint space, by using the Lagrange equation [3]. The equation of motion in matrix form can be written as:

$$D(q)\ddot{q} + C(q, \dot{q})\dot{q} + F_s \operatorname{sgn}(\dot{q}) + g(q) = \tau \quad (1)$$

In this expression,  $q$  is the vector of joint angles,  $D(q)$  is the inertia matrix,  $C(q, \dot{q})$  is the vector of centripetal and Coriolis forces,  $F_s$  is an approximated friction forces,  $\operatorname{sgn}(\cdot)$  is the signum function,  $g(q)$  is the vector of gravitational forces and  $\tau$  is the torque vector applied to the joints. For this system, each matrix in the dynamic equations can be written as:

$$D(q) = \begin{bmatrix} I_{1_{22}} + I_{2_{11}} \sin^2 q_2 + I_{2_{33}} \cos^2 q_2 & 0 \\ 0 & I_{2_{22}} \end{bmatrix}$$

$$C(q, \dot{q}) = \begin{bmatrix} \frac{1}{2} \dot{q}_2 (I_{2_{11}} - I_{2_{33}}) \times \sin(2q_2) & \frac{1}{2} \dot{q}_1 (I_{2_{11}} - I_{2_{33}}) \times \sin(2q_2) \\ -\frac{1}{2} \dot{q}_1 (I_{2_{11}} - I_{2_{33}}) \times \sin(2q_2) & 0 \end{bmatrix}$$

where  $I_{i_{jk}}$  is a member of row  $j$  and column  $k$  of moment of inertia of link  $i$ .

$$I_1 = \begin{bmatrix} 0.065 & 0 & 0 \\ 0 & 0.069 & 0 \\ 0 & 0 & 0.07 \end{bmatrix}, I_2 = \begin{bmatrix} 0.018 & 0 & 0 \\ 0 & 0.024 & 0 \\ 0 & 0 & 0.025 \end{bmatrix}$$

$I_1$  and  $I_2$  can be obtained by computer aided design software.

## 3. The Controller Design

Combined feedforward plus feedback control can significantly improve performance over simple feedback control whenever there is a major disturbance that can be measured before it affects the process output. In the most ideal situation, feedforward control can entirely eliminate the effect of the measured disturbance on the process output. Even when there are modeling errors, feedforward control can often reduce the effect of the measured disturbance on the output better than that achievable by feedback control alone.

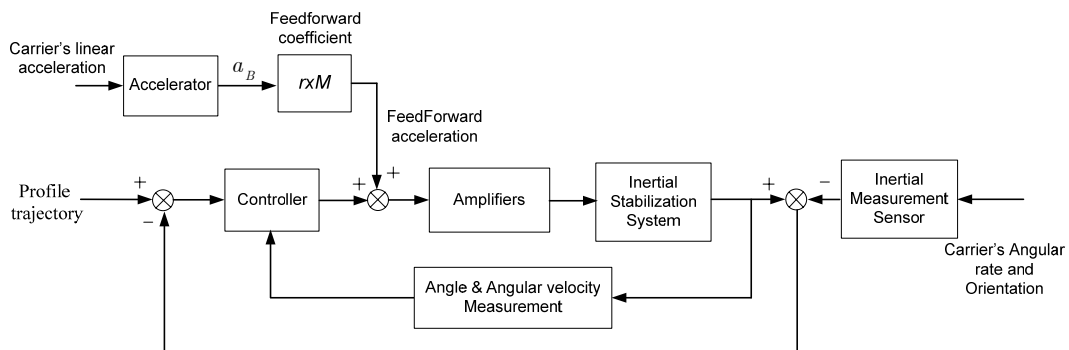


Fig. 3 Motion control diagram with acceleration feedforward

In the motion control diagram as Fig.3, the plant is driven by the feedforward. The feedback loop consists of a controller, two power amplifiers, a plant and inertial measurement sensor. The controller consists of robust inverse dynamics control and indirect line of sight stabilization.

### 3.1 Robust Inverse Dynamics Control

This system is a nonlinear multivariable system. The controller technique called inverse dynamics control can be used to obtain the global linearization of the system dynamics. The dynamic equation of this system is expressed by Eq. (1) which can be rewritten as

$$\tau = \mathbf{D}(q)y + \mathbf{N}(q, \dot{q}) \quad (2)$$

where  $\mathbf{N}(q, \dot{q}) = \mathbf{C}(q, \dot{q})\dot{q} + \mathbf{F}_s \text{sgn}(\dot{q}) + \mathbf{g}(q)$ .

And  $y$  can be selected as:

$$y = \ddot{q}_d + K_P \tilde{q} + K_D \dot{\tilde{q}} + K_I \int_0^t \tilde{q} dt \quad (3)$$

where  $q_d, \dot{q}_d, \ddot{q}_d$  are the desired joint trajectory, joint velocity, and joint acceleration.  $\tilde{q} = q_d - q$  expresses the dynamics of position error, while tracking the given trajectory,  $q_d, \dot{q}_d, \ddot{q}_d$ . The gain  $K_P, K_D, K_I$  can be selected by specifying the desired speed of response.

Referring to Eq. (2), in the presence of uncertainties including modeling errors, unknown loads, and parameters measurement, the control vector is expressed by

$$\tau = \hat{\mathbf{D}}(q)y + \hat{\mathbf{N}}(q, \dot{q}) \quad (4)$$

where  $y$  is a new input vector to be determined,  $\hat{\mathbf{D}}(q)$  and  $\hat{\mathbf{N}}(q, \dot{q})$  denote the estimators of the inertial matrix  $\mathbf{D}(q)$  and the nonlinear coupling matrix  $\mathbf{N}(q, \dot{q})$  implemented in the controller, respectively.

Taking Eq. (4) as a nonlinear control law gives

$$\mathbf{D}(q)\ddot{q} + \mathbf{N}(q, \dot{q}) = \hat{\mathbf{D}}(q)y + \hat{\mathbf{N}}(q, \dot{q}) \quad (5)$$

which allows the generation of

$$\begin{aligned} \ddot{q} &= y + (\mathbf{D}^{-1}(q)\hat{\mathbf{D}}(q) - \mathbf{I})y + \mathbf{D}^{-1}(\hat{\mathbf{N}}(q, \dot{q}) - \mathbf{N}(q, \dot{q})) \\ &= y - \Gamma \end{aligned} \quad (6)$$

where  $\mathbf{I}$  denotes a  $3 \times 3$  identity matrix and

$$\Gamma = (\mathbf{I} - \mathbf{D}^{-1}(q)\hat{\mathbf{D}}(q))y - \mathbf{D}^{-1}(\hat{\mathbf{N}}(q, \dot{q}) - \mathbf{N}(q, \dot{q})) \quad (7)$$

From Eq. (6) can be rewritten as:

$$\ddot{q}_d - \ddot{q} = \ddot{q}_d - y + \Gamma \rightarrow \ddot{\tilde{q}} = \ddot{q}_d - y + \Gamma \quad (8)$$

Let define state variables as  $\eta = \begin{bmatrix} \tilde{q} \\ \dot{\tilde{q}} \end{bmatrix}$

The state equation of Eq. (6) can be written as:

$$\begin{bmatrix} \dot{\eta} \\ \ddot{\eta} \end{bmatrix} = \begin{bmatrix} 0 & \mathbf{I} \\ 0 & 0 \end{bmatrix} \begin{bmatrix} \eta \\ \dot{\eta} \end{bmatrix} + \begin{bmatrix} 0 \\ \mathbf{I} \end{bmatrix} (\ddot{q}_d - y + \Gamma) \quad (9)$$

In order to compensate for the uncertainties, the following input vector  $y$  is chosen:

$$y = \ddot{q}_d + K_D \dot{\tilde{q}} + K_P \tilde{q} + K_I \int_0^t \tilde{q} dt + w \quad (10)$$

The term  $w$  is an additional item to be designed to guarantee robustness to the effects of uncertainties described by  $\Gamma$  in Eq. (7).

Substitute Eq. (10) into Eq. (9), we get:

$$\begin{aligned} \begin{bmatrix} \dot{\eta} \\ \ddot{\eta} \\ \dot{\beta} \end{bmatrix} &= \begin{bmatrix} 0 & \mathbf{I} \\ 0 & 0 \end{bmatrix} \begin{bmatrix} \eta \\ \dot{\eta} \end{bmatrix} + \begin{bmatrix} 0 \\ \mathbf{I} \end{bmatrix} \left( -K_P \tilde{q} - K_D \dot{\tilde{q}} - K_I \int_0^t \tilde{q} dt - w + \Gamma \right) \\ \begin{bmatrix} \dot{\eta} \\ \ddot{\eta} \\ \dot{\beta} \end{bmatrix} &= \begin{bmatrix} 0 & \mathbf{I} & 0 \\ -K_P & -K_D & -K_I \\ \mathbf{I} & 0 & 0 \end{bmatrix} \begin{bmatrix} \eta \\ \dot{\eta} \\ \beta \end{bmatrix} + \begin{bmatrix} 0 \\ \mathbf{I} \\ 0 \end{bmatrix} (\Gamma - w) \\ \dot{\zeta} &= \mathbf{H}\zeta + \mathbf{G}(\Gamma - w) \end{aligned} \quad (11)$$

where

$$\beta = \int_0^t \tilde{q} dt, \quad \zeta = \begin{bmatrix} \eta \\ \dot{\eta} \\ \beta \end{bmatrix}, \quad \mathbf{H} = \begin{bmatrix} 0 & \mathbf{I} & 0 \\ -K_P & -K_D & -K_I \\ \mathbf{I} & 0 & 0 \end{bmatrix},$$

$$\text{and } \mathbf{G} = \begin{bmatrix} 0 \\ \mathbf{I} \\ 0 \end{bmatrix}$$

For this system,  $\zeta$  is a  $6 \times 1$  vector. Since the matrices  $K_P, K_D$  and  $K_I$  are chosen so that  $\mathbf{H}$  in Eq. (11) is a Hurwitz matrix, i.e.,  $\mathbf{H}$  has all its eigen values with all negative real parts.

To determine  $w$ , consider the positive definite quadratic from Lyapunov function candidate.

$$V = \zeta^T \mathbf{Q} \zeta > 0 \quad \forall \zeta \neq 0 \quad (12)$$

where  $\mathbf{Q}$  is a symmetric positive definite matrix

$$\dot{V} = \zeta^T \mathbf{Q} \dot{\zeta} + \dot{\zeta}^T \mathbf{Q} \zeta \quad (13)$$

$$\dot{V} = \zeta^T (\mathbf{H}^T \mathbf{Q} + \mathbf{Q} \mathbf{H}) \zeta + 2\zeta^T \mathbf{Q} \mathbf{G} (\Gamma - w) \quad (14)$$

Because  $\mathbf{H}$  has negative eigenvalues, any symmetric positive definite matrix  $\mathbf{P}$  can be chosen to give a unique solution  $\mathbf{Q}$  satisfying the relationship:

$$(\mathbf{H}^T \mathbf{Q} + \mathbf{Q} \mathbf{H}) = -\mathbf{P} \quad (15)$$

So, Eq. (14) becomes:

$$\dot{V} = -\zeta^T \mathbf{P} \zeta + 2\zeta^T \mathbf{Q} \mathbf{G} (\Gamma - w) \quad (16)$$

To make  $\dot{V}$  negative definite, we will need  $\|w\| \geq \|I\|$ . So, it will be true that:

$$w = \frac{\rho}{\|G^T Q \zeta\|} (G^T Q \zeta), \quad \rho \geq \|I\| \quad (17a)$$

For small value of  $\|G^T Q \zeta\| < \varepsilon$ , Eq. (17a) will be modified to:

$$w = \frac{\rho}{\varepsilon} (G^T Q \zeta), \quad \|G^T Q \zeta\| < \varepsilon \quad (17b)$$

The Eq. (17b) is to prevent chattering.

### 3.2 Acceleration feedforward

The main objective of the motion control is to control the angle and angular velocity of the joints to a desired state by measurements of the angle and angular velocity only. For cancellation the disturbance due to motion of the airplane, a rate sensor is mounted on the base of the gimbal to measure base rate. The base rate will be transformed to LOS (line of sight) coordinate. The controller will compute command to reject this disturbance. By introducing an acceleration feedback, such effects can be caught at an earlier stage since the force disturbance is sensed directly.

#### 3.2.1 Rotation matrices

The gimbal consists of two revolute joints which powered by DC-motor. The camera is located on the center of the two axes as shown in Fig. 4. In order to describe the orientation of the gimbal, we will attach three coordinate systems to the gimbal. There are three coordinate frames needed to be defined are the gimbal base frame (B), the gimbal outer frame or Azimuth (A), and the gimbal inner frame or Elevation (E).

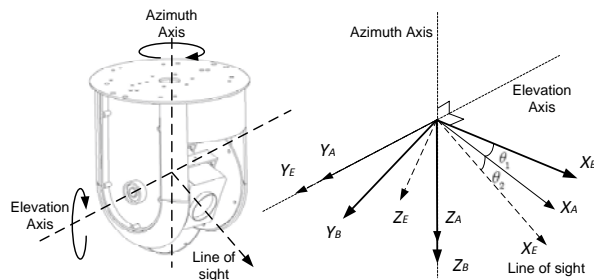


Fig. 4 Link Frame Assignment

The base frame fixed (B) to the body of the carrier with its  $X_B$  axis heading forward and  $Y_B$  to the right side of the gimbal. The coordinate frame (A) attached to the outer gimbal (azimuth axis), which can rotate with respect to the carrier around the  $Z_B$  and  $Z_A$  axis and finally the coordinate frame (E) attached to the inner gimbal (elevation axis), which can rotate with respect to the azimuth gimbal around the  $Y_A$  and  $Y_E$  axis.

The rotation matrix of the outer gimbal (azimuth axis) respect to the gimbal base frame is expressed as

$$R_B^A = \begin{bmatrix} \cos \theta_1 & \sin \theta_1 & 0 \\ -\sin \theta_1 & \cos \theta_1 & 0 \\ 0 & 0 & 1 \end{bmatrix} \quad (18)$$

The rotation matrix of the gimbal inner frame respect to the outer gimbal is expressed as

$$R_A^E = \begin{bmatrix} \cos \theta_2 & 0 & -\sin \theta_2 \\ 0 & 1 & 0 \\ \sin \theta_2 & 0 & \cos \theta_2 \end{bmatrix} \quad (19)$$

The composition of two rotations is

$$R_B^E = R_A^E R_B^A = \begin{bmatrix} \cos \theta_1 \cos \theta_2 & \sin \theta_1 \cos \theta_2 & -\sin \theta_2 \\ -\sin \theta_1 & \cos \theta_1 & 0 \\ \cos \theta_1 \sin \theta_2 & \sin \theta_1 \sin \theta_2 & \cos \theta_2 \end{bmatrix} \quad (20)$$

#### 3.2.2 The disturbance torque

From these rotation matrices, the acceleration of the outer gimbal respect to the gimbal base is expressed as.

$$a_A = R_B^A a_B \quad (21)$$

The acceleration  $a_A$  generates the disturbance torque  $T_{AZ}$  around the azimuth axis  $Z_A$ , is consisted of two component

$$T_{AZ} = [r_A \times M_A a_A]_Z + [r_{EA}(\theta) \times M_E a_A]_Z \quad (22)$$

where the first component is the unbalance of the outer gimbal described by the mass of the outer gimbal  $M_A$  and the vector of the center of mass  $r_A$ , and the second component represents the unbalance of the inner gimbal described by the total mass of the inner gimbal  $M_E$  and the distance from the elevation gimbal center of mass to the azimuth joint axis.

And the acceleration of the inner gimbal is

$$a_E = R_B^E a_B \quad (23)$$

Consider unbalance mass system revolved around a central axis  $O$ , as shown in Fig. 1. The disturbance torque around the elevation axis  $Y_E$  in the gimbal inner frame, which generated by the acceleration  $a_E$  of the center of gravity of the inner gimbal, is expressed as

$$T_{EY} = [r_E \times M_E a_E]_Y \\ = [r_E \times M_E R_B^E a_B]_Y \quad (24)$$

where  $r_E$  is a displacement vector of the center of mass.

For the field work, the gimbal is mounted on the platform under the helicopter, as illustrated in Fig. 5. The vibrations of the helicopter are passed to the platform and give rise to a more disturbance torque. When the helicopter resides

still on the ground, the mass unbalance leads to a periodic disturbance torque acting on the camera.



Fig.5 The gimbal mounted on the helicopter

### 3.3. Combination of feedforward and feedback control

Fig. 6 shows the block diagram of the robust inverse dynamic control and acceleration feedforward. An inertial measurement sensor is added to detect vehicle angular rate and orientation for outer loop control and an accelerometer is added to detect vehicle's linear acceleration.

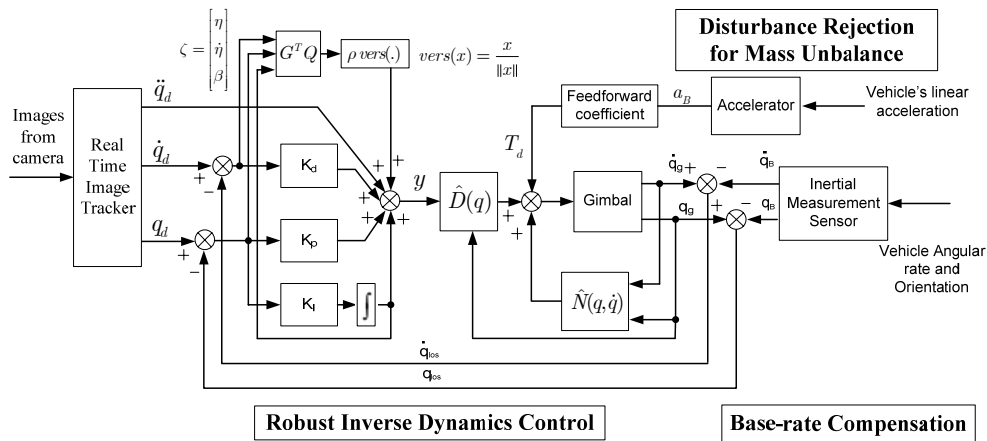


Fig. 6 The block diagram of the controller

### 4. Experiment result

In laboratory, the experimental setup is shown in Fig.7. The gimbal is hung freely on the trust frame. A gyro enhanced orientation sensor is mounted on the base of the gimbal. These experiments focus on the controller, only acceleration feedforward in the gimbal inner frame (elevation axis  $y_E$ ). To demonstrate the performance of the controllers mentioned in this paper, the base of gimbal allows for a vertical motion with the amplitude of several centimeters while maintaining its LOS direction.



Fig. 7 Environment Setup

$q_d, \dot{q}_d, \ddot{q}_d$  is generated from the trapezoidal velocity profile or s-profile trajectory. A trapezoidal velocity profile is generated by setting traveling distance, maximum velocity, and maximum acceleration equal to 1 rad, 0.5 rad/sec, and 0.8 rad/sec<sup>2</sup> respectively.

For the first case, the response of pitch angle for robust inverse dynamic and robust inverse dynamic control with acceleration feedforward are shown in Fig. 8 – 13

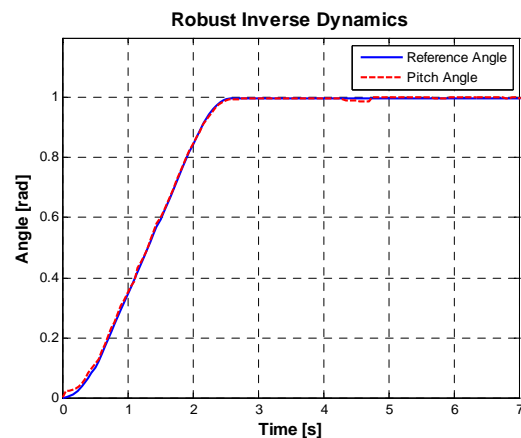


Fig. 8 The response of robust inverse dynamics control

First, the disturbance is added while the gimbal is moving to the new target. To test the tracking capability, the reference trajectory

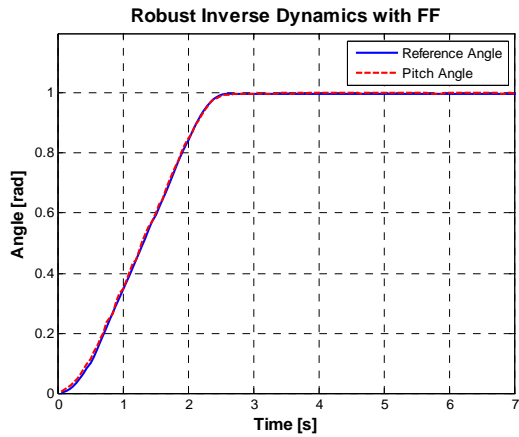


Fig. 9 The response of robust inverse dynamics control with FF

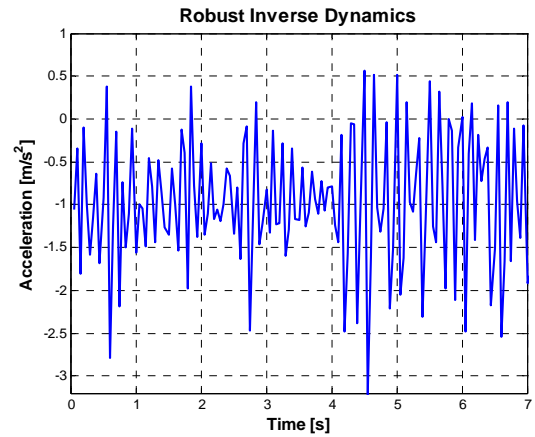


Fig. 12: Vibration in Z Axis of robust inverse dynamics control

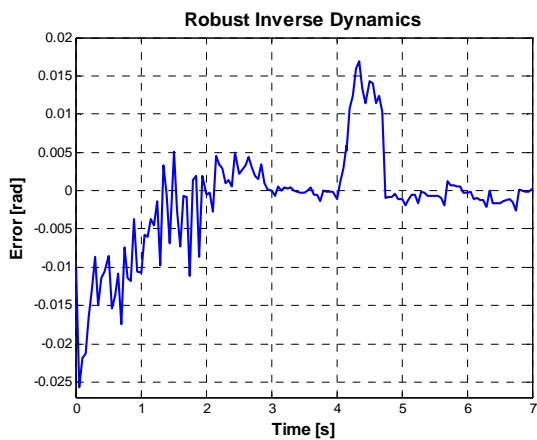


Fig. 10: Error of the tracking of robust inverse dynamics control

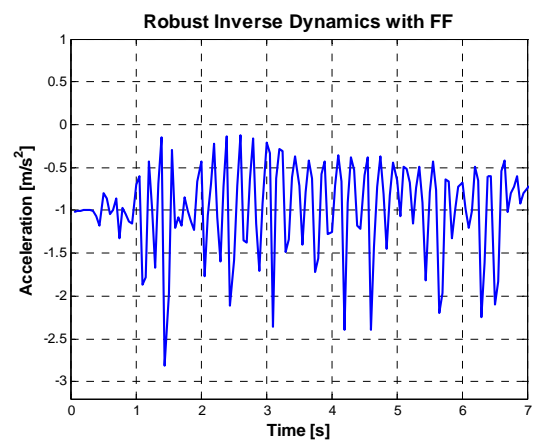


Fig. 13: Vibration in Z Axis of robust inverse dynamics control with FF

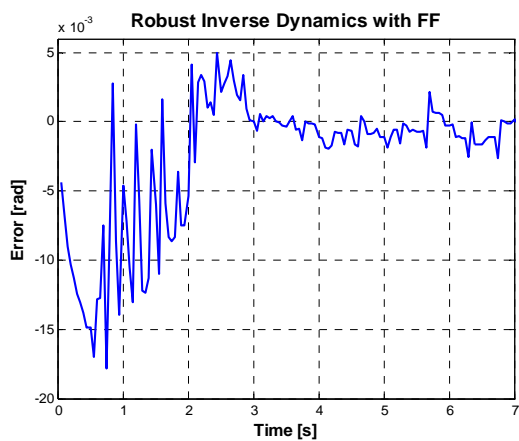


Fig. 11: Error of the tracking of robust inverse dynamics control with FF

For the second experiment, we create a reference command close to the real situation. The reference command will be a sinusoidal function. The response of the pitch axis for the robust inverse dynamic and the acceleration feedforward compensation are shown in Fig. 14 - 19.

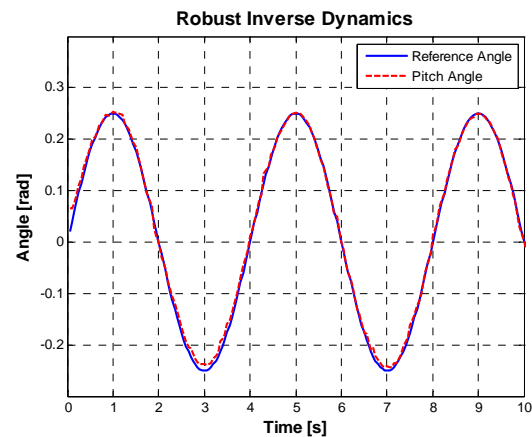


Fig. 14 The response of robust inverse dynamics control

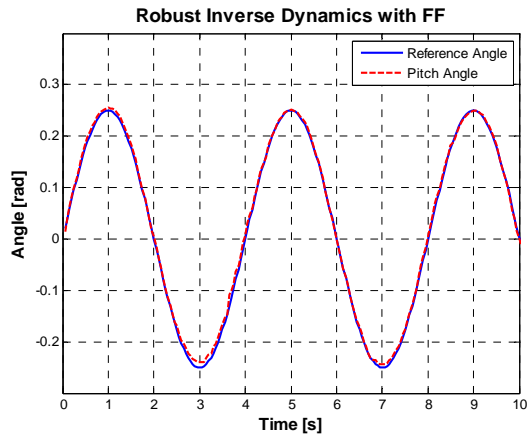


Fig. 15 The response of robust inverse dynamics control with FF

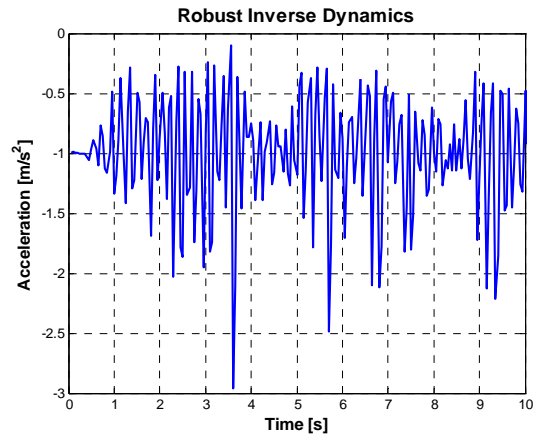


Fig. 18: Vibration in Z Axis of robust inverse dynamics control

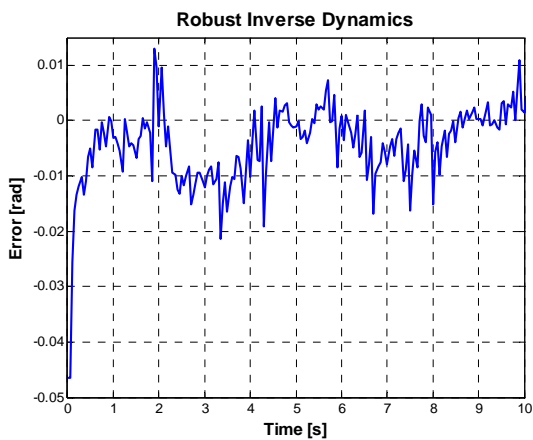


Fig. 16: Error of the tracking of robust inverse dynamics control

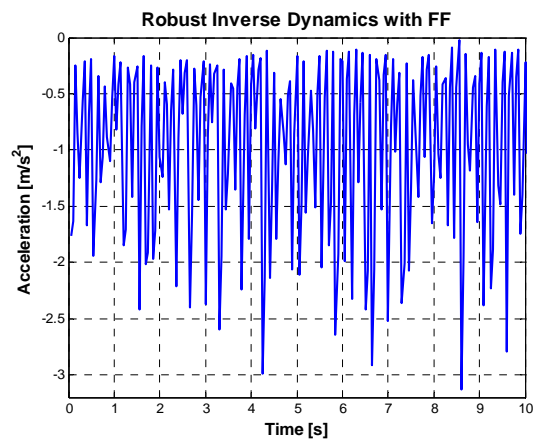


Fig. 19: Vibration in Z Axis of robust inverse dynamics control with FF

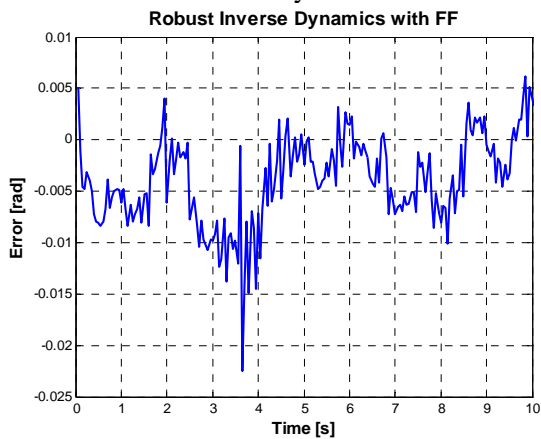


Fig. 17: Error of the tracking of robust inverse dynamics control with FF

The experimental results show that the robust inverse dynamics control with the acceleration feedforward compensation verifies the effectiveness of the method in rejecting base disturbances.

### 5. Conclusion

In this paper, we have designed controllers to satisfy stabilization performance of a two-axis gimbal system. The details of the two controllers, the robust inverse dynamic and acceleration feedforward, are described. The robust inverse dynamic and acceleration feedforward can be used for trajectory tracking in the presence of dynamics uncertainties. Indirect stabilization and acceleration feedforward are reducing the jittering due to base rate disturbances. Unbalanced mass can also be compensated by acceleration feedforward action. The experiment results in the two-axes gimbal is presented to verify the effectiveness of the proposed method in rejecting carrier disturbances. The controllers perform very effective for this system.

## 6. Acknowledgement

Part of this work is sponsored by Chulalongkorn University under Chulalongkorn University Centenary Academic Development Project.

## 7. References

- [1] Peter, J. K. (2003). Direct Versus Indirect Line of Sight (LOS) Stabilization, *IEEE Transactions on Control Systems Technology*, vol. 11(1), January 2003, pp. 3 – 15.
- [2] Masten, M. (2008). Inertially stabilized platforms for optical imaging systems: Tracking dynamic dynamic targets with mobile sensors, *Control Systems Magazine, IEEE*, vol. 28, February 2008, pp. 47–64
- [3] Sangveraphunsiri, V. and Malithong, K. (2009). Robust Inverse Dynamics and Sliding Mode Control for Inertial Stabilization Systems, *Asian International Journal of Science and Technology in Production and Manufacturing Engineering*, vol. 2(4), October - December , 2009, pp. 33–45
- [4] Wei, J., Qi, L. and Bo, X. (2006). Design Study of Adaptive Fuzzy PID Controller for LOS Stabilized System, paper presented in *the Sixth International Conference on Intelligent Systems Design and Applications*, Washington, DC, USA
- [5] Bo, L., David, H. and Mike, D. (1998) Nonlinear Induced Disturbance Rejection in Inertial Stabilization Systems, *IEEE Transactions on Control Systems Technology*, vol. 6(3), May 1998, pp. 421 - 427
- [6] Lorenzo, S., Bruno, S. (1996) *Modeling and Control of Robot Manipulators*. , International edition, ISBN 0-07-114726-8, The McGraw-Hill Companies, Inc., Singapore,